Upregulation of circ_0000069 stimulates cervical cancer development by enhancing proliferation, migration, invasion while inhibiting apoptosis through the miR-4429/ZIC2 axis

Hongjuan Yang
The Affiliated Hospital of Qingdao University
Xiangkun Li
The Affiliated Hospital of Qingdao University
Xinwei Zhao
Qingdao Huangdao District Central Hospital
Chang Wang
The Affiliated Hospital of Qingdao University
Dongyan Qin
The Affiliated Hospital of Qingdao University
Dongmei Gao
The Affiliated Hospital of Qingdao University
Jinwen Jiao (zxbr7ix@163.com)
The Affiliated Hospital of Qingdao University https://orcid.org/0000-0001-9941-4884

Primary research

Keywords: circ_0000069, miR-4429, ZIC2, CC

Posted Date: February 21st, 2020

DOI: https://doi.org/10.21203/rs.2.24151/v1

Abstract

Background Cervical cancer (CC) is a common female cancer according to global cancer statistics. The current study was used to investigate the regulatory mechanism of circ_0000069 in CC. Methods The real-time quantitative polymerase chain reaction (RT-qPCR) was used to assess circ_0000069, miR-4429, and zinc finger protein of the cerebellum 2 (ZIC2) expression in CC tissues and cells. Kaplan-Meier analysis was performed in CC patients to analyze the relationship between survival time and circ_0000069 expression. The proliferation, apoptosis, cell cycle of CC cells were detected by 3-(4, 5-dimethylthiazol-2-yl)-2, 5-diphenyl-2H-tetrazol-3-ium bromide (MTT), colony formation, and flow cytometry analyses, respectively. In addition, western blot assay was employed to show expression levels of apoptosis/cell cycle-related proteins, as well as ZIC2. The migration and invasion of CC cells were assessed by transwell analysis. Possible target miRNAs of circ_0000069, along with the interaction between ZIC2 and miR-4429 were confirmed by pull-down and dual-luciferase reporter assays. Eventually, the functional role of circ_0000069 in vivo was clarified with the xenograft experiment in nude mice. Results Circ_0000069 was overexpressed in CC tissues and cells than controls. Furthermore, the silencing of circ_0000069 inhibited proliferation, migration, and invasion while included apoptosis and cell cycle arrest of CC cells, which was overturned by downregulation of miR-4429. Importantly, ZIC2 was a direct target of miR-4429 in CC cells, and we further confirmed that overexpression of miR-4429 suppressed CC progress by decreasing ZIC2 expression in CC cells. Surely, silencing of circ_0000069 inhibited tumorigenesis in vivo. Conclusion Our current results suggested that circ_0000069 exerted its tumorigenic roles by regulation of proliferation, apoptosis, cell cycle, migration, and invasion of CC cells, supporting that circ_0000069/miR-4429/ZIC2 axis may provide potential prognostic biomarkers for CC.

Background

Cervical cancer (CC) ranks fourth for both incidence and cancer-related death in women according to global cancer statistics 2018 [1]. The metastasis and easy recurrence were major obstacles for improving the survival time of CC patients [2, 3]. Therefore, further molecular research on the fundamental mechanism of CC development was meaningful, which may provide a new treatment strategy for CC patients.

Circular RNAs (circRNAs) are new members of the non-coding RNAs with covalently linked ends, generating from back-splicing of exons in various cell lines and across different species [4, 5]. Emerging evidence has indicated that circRNAs could function as crucial mediators to participate in initiation and development of multiple diseases [6]. For example, circ_0000069 was derived from the SCL/TAL1 interrupting locus (STIL) gene and located on chr1 (47745912-47748131). Circ_0000069 was reported to be associate with worse clinical outcome of colorectal cancer patients [7]. As far as we know, few studies focused on the function and regulator mechanism of circ_0000069 in CC.

MicroRNAs(miRNAs), non-coding RNAs with 18-22 nucleotides in length, was implicated in cervical carcinogenesis [8]. It had been reported that miRNAs caused mRNA degradation by targeting the 3’ untranslated region (3’UTR) [9]. Recently, the anti-oncogenic role of miR-4429 has been confirmed in clear cell renal cell carcinoma [10]. Furthermore, miR-4429 was differentially downregulated in CC cells when compared to normal cells [11]. The potential role of miR-4429 in CC was further investigated in the current study.

Zinc finger protein of the cerebellum 2 (ZIC2), transcription factors, was a member of ZIC family, involving in vertebrate development [12], oncogenesis [13], and transcriptional regulation [14]. Recent studies reported that ZIC2 acted as an oncogene in breast cancer [15]. Interestingly, Chan *et al*. revealed that overexpression of ZIC2 in CC cells obviously increased cell proliferation and metastasis abilities [16]. Consequently, a previous study suggested that the downregulation of ZIC2 inhibited the invasion potential of nasopharyngeal carcinoma cells [17].

Based on those findings, our investigation focused on the implications and roles of circ_0000069 in CC. We aimed to demonstrate the association relationship among circ_0000069, miR-4429, and ZIC2 network in the development of CC, which may provide potential novel targets for CC therapeutics.

Materials And Methods

Patient specimens

In the total of 62 paired samples of CC and neighboring non-tumorous tissues were harvested from CC patients with prior written informed consent from the patients at The Affiliated Hospital of Qingdao University. All tissues were confirmed as CC samples by two pathologists following surgery and then frozen in liquid nitrogen. Sample tissues were transferred to a -80℃ refrigerator until total RNA or protein extraction. Patients with CC were assigned to two groups (I+II group and III+ IV groups) according to the patient's clinical stage. In addition, CC patients were divided into high (n=31) and low (n=31) circ_0000069 expression groups with median circ_0000069 expression value as the cutoff. The correlations between hsa_circ_0000069 expression and clinical characteristics of cervical cancer patients were listed in Table 1. All the procedures were permitted by the Ethics Committee of The Affiliated Hospital of Qingdao University.

Cell culture

The normal cervical epithelial cells (HcerEpic) were bought from the Chinese Academy of Sciences Cell Bank (Shanghai, China). In addition, CC cell lines (HeLa and SW756) were acquired from the American Type Culture Collection (Rockville, MD, USA). The above cells were maintained in RPMI1640 media (Invitrogen, Carlsbad, CA, USA) supplemented with 10% fetal bovine serum (FBS; Invitrogen) and antibodies (penicillin/streptomycin; Invitrogen) in a humidified atmosphere containing 5% CO_2 at 37℃.

RNA isolation and real-time quantitative polymerase chain reaction (RT-qPCR)

RT-qPCR assay was conducted to determine RNA level in cells and tumor tissues. In brief, total RNA was isolated by TRIzol Kit (Vazyme Biotech, Nanjing, China) as instructed by the manufacturer. For quantitation with circRNA and mRNA, complementary DNA (cDNA) was synthesized by High-capacity cDNA Reverse Transcription kit (Bio-Rad, Hercules, CA, USA). The transcript levels of target genes were measured by SYBR Fast qPCR Mix (Thermo Fisher Scientific, Waltham, MA, USA) under AB7300 thermo-recycler (Applied Biosystems, Carlsbad, CA, USA) and normalized to glyceraldehyde-3-phosphate dehydrogenase (GAPDH) by using $2^{-\Delta\Delta Ct}$ method. As for miR-4429, total RNA was reversedly transcribed to cDNA using TaqMan Reverse Transcription Kit (Applied Biosystems) according to the manufacturers' instructions. TaqMan MicroRNA Assays Kit (Applied Biosystems) was used to quantify the expression level of miR-4429 in cells or tissues, with

small nuclear RNA U6 as an internal control. Moreover, partial total RNA was treated with RNase R (3U/mg: Epicentre Technologies, Madison, WI, USA) at 37℃ for 15 min for RNase R treatment assay.

The sequences of partial primers were listed:

circ_0000069 (Forward (F)-5'-CTACTTCAGGCACAGGTCTTC-3'; Reverse (R)-5'-CTGACTCACTGGATGAGGACT-3');

STIL (F-5'-CCCAACGCCAACTGGAGATTT-3'; R-5'-AGTCGGATGGTCTTCTCAGTC -3');

miR-4429 (F-5'-GCCGAGAAAAGCTGGGCTGAG-3'; R-5'- CTCAACTGGTGTCGTGGA-3');

ZIC2 (F-5'-GCGCAACTCCACAACCAGTA-3'; R-5'-TGCCGCATATAGCGGAAAAAG-3');

GAPDH (F-5'-TCCCATCACCATCTTCCAGG-3'; R-5'-GATGACCCTTTTGGCTCCC-3');

U6 (F-5'-AACGCTTCACGAATTTGCGT-3'; R-5'- CTCGCTTCGGCAGCACA-3').

Transfection assay

Small interfering RNA (siRNA) against circ_0000069 (si-circ_0000069) and siRNA control (si-NC), miR-4429 mimic (miR-4429) and its control (miR-NC), and miR-4429 inhibitor (anti-miR-4429) and its control (anti-miR-NC) were generated by Sangon (Shanghai, China). Furthermore, circ_0000069-overexpression vector (circ_0000069), ZIC2-overexpression vector (ZIC2) and their control (vector) were obtained from Genomeditech (Shanghai, China). For transfection assay, 1×10^5 cells were seeded into 12-well plates and allowed to attach. After culture overnight, Lipofectamine 2000 (Invitrogen) reagent and 150 ng of siRNA, 1 μg of plasmids, or 80 nM of miRNA mimic/inhibitor were mixed and then added to the cells.

Cell proliferation assay

For 3-(4, 5-dimethylthiazol-2-yl)-2, 5-diphenyl-2H-tetrazol-3-ium bromide (MTT) assay, HeLa and SW756 cells were seeded in 96 wells (3000 cells per well). After incubation for the indicated time, 20 μL of MTT (Promega, Madison, WI, USA) was added to cells and then incubated for another 4 h. After discarding the medium, 150 μL of dimethyl sulfoxide (DMSO) was administrated to cells. We reported the cell viability every 12 h by detecting optical density at wavelength of 490 nm each well on microplate reader (Bio-Rad). For colony formation assay, briefly, HeLa and SW756 cells were seeded in 96 wells (500 cells per well) and routinely cultured for two weeks. Then the colonies were fastened with 4% formaldehyde for 10 min and dyed with 0.1% crystal violet. Cell colonies were counted and photographed.

Apoptosis and cell cycle

For cell apoptosis analysis was conducted by using an Annexin V labeled with fluorescein isothiocyanate (FITC) Apoptosis Detection Kit I (Thermo Fisher Scientific) following the manufacturer's recommended instructions. HeLa and SW756 cells were collected by trypsin and then re-suspended in binding buffer supplemented with 5 μL of Annexin V labeled with FITC and 5 μL of propidium iodide (PI). After incubation for 20 min, apoptotic cells were monitored by flow cytometry (Applied Biosystems). Apoptosis rate = (Annexin

V^+PI^+ cell numbers + Annexin V^+PI^- cell numbers)/total cells×100%). For cell cycle detection, 100 uL of cell suspension ($1×10^6$/mL) was treated with PI staining solution contained RNase R and TritonX-100 for 30 min at 4°C, then flow cytometry was conducted to detect cell cycle distribution.

Western blot assay

Briefly, proteins were segregated on 10% sodium dodecyl sulfate polyacrylamide gels. The isolated proteins were subjected to wet electrophoretic transfer method and then transferred onto polyvinylidene fluoride membranes (Millipore, Billerica, MA, USA). The membranes were incubated with 5% non-fat milk followed by incubation with the primary antibodies at 4°C overnight. After being washed, membranes interacted with horseradish peroxidase-conjugated Goat polyclonal Antibody to Rabbit (ab150077; 1:3000 dilution; Abcam, Cambridge, MA, USA) for 1 h. Antibody binding was visualized with Western Blotting Detection Kit (Solarbio, Beijing, China) under Alpha Innotech Imaging System (Protein Simple, Santa Clara, CA, USA). The primary antibodies were listed as followed: anti-B-cell lymphoma-2 (Bcl-2; ab32124; 1:1000 dilution; Abcam), anti-Bcl-2-associated x (Bax; ab32503; 1:1000 dilution; Abcam), anti-cyclin-dependent kinases2 (CDK2; ab32147; 1:1000 dilution; Abcam), anti-cyclin-dependent kinases4 (CDK4; ab108357; 1:1000 dilution; Abcam), anti-ZIC2 (ab150404; 1:1000 dilution; Abcam), and anti-GAPDH (ab181602; 1:3000 dilution; Abcam).

Transwell assay

For the migration assay, $5×10^4$ CC cells were plated in the top chamber of 24-well transwell chamber (6 well insert, 8 μm pore size). Notably, the top chamber of transwell chamber was pro-adhered with Matrigel (Becton Dickinson, San Jose, CA, USA) for transwell invasion assay. The complete medium contained with 10% fetal bovine serum was added into the lower chamber of transwell chamber as chemoattractant. After 24 h of incubation, cells that migrated or invaded were fastened with 4% formaldehyde and dyed with 0.1% crystal violet. Eventually, a microscope (Olympus Corp, Tokyo, Japan) was used to count cell numbers of migrated or invaded cells in five random visual fields.

Biotinylated RNA pull-down assay

The magnetic beads (Life Technologies, Carlsbad, CA, USA) pro-covered with circ_0000069 probe were incubated with cell lysates from HeLa and SW756 cells at 4°Covernight. After pull-down assay, immunoprecipitated RNA was extracted by TRIzol Kit and then subjected to RT-qPCR assay. In particular, for analysis of the relationship between miR-4429 and circ_0000069, HeLa and SW756 cells were infected with biotinylated miR-4429 mimics or mutant (Biotin-miR-4429-WT and Biotin-miR-4429-MUT; designed by Sangon) using Lipofectamine 2000. After 48 h, HeLa and SW756 cells were collected, lysed, and then incubated with streptavidin-coupled magnetic beads to generate biotin-coupled RNA complex. The expression level of circ_0000069 was analyzed by RT-qPCR assay.

Dual-luciferase reporter assay

The bioinformatics databases starbase (http://starbase.sysu.edu.cn/) and circBank (http://www.circbank.cn/) bioinformatics databases were utilized to forecast target miRNA of circ_0000069. Furthermore, the complementary sites between miR-4429 and 3'UTR of ZIC2 were predicted by bioinformatics databases

starbase. The fragments of circ_0000069 or 3’ UTR of ZIC2 were amplified by RCR and then cloned into pGL3 vectors (Promega), named as circ_0000069 WT and ZIC2 3’-UTR-WT, respectively. In addition, mutant of circ_0000069 or 3’ UTR of ZIC2 was constructed with KOD-plus-mutagenesis kit (Toyobo, Osaka, Japan). After that, 80 nM of miR-4429 mimic or miR-NC were co-transfected with 0.5 μg of reporter vector using Lipofectamine 2000. The relative firefly luciferase activity was checked by Dual-Luciferase Assay Kit (GeneCopoeia, Rockville, MD, USA) and standardized to renilla luciferase signal.

In vivo experiment

For the animal experiments, HeLa cells were stably transfected with lentiviral vectors with short hairpin RNAs (shRNAs) targeting circ_0000069 (sh-circ_0000069) or control (sh-NC) constructed by GeneCopoeia. The 12 BALB/c nude mice (Shanghai Experimental Animal Center, Shanghai, China) were randomly divided into 2 groups. 2×10^6 HeLa cells in 200 μL of FBS-free culture medium were hypodermically vaccinated into left flank near the forelimb of BALB/c nude mice, while sh-NC was served as control group. Tumor volume was measured every 3 d based on $V = 1/2\times ab^2$ method (length (a) and width (b) length of the tumor). All mice were sacrificed by cervical dislocation on 21 d, and the tumors tissues were collected for subsequent experiments. The animal experiments were approved by the Institutional Animal Care and Use Committee of The Affiliated Hospital of Qingdao University.

Statistical analysis

All data were exhibited as mean ± standard deviation from at least 3 times independent experiments, and P <0.05 was considered statistically significant. All analyses were carried out using the SPSS 21.0 software (IBM, Somers, NY, USA) based on Student’s *t*-test and one-way analysis of variance. In addition, the survival curves of CC patients were plotted using the Kaplan-Meier method and the log-rank test. The correlation between clinicopathological characteristics of CC patients and circ_0000069 expression was assessed by Chi-square test. Pearson’s correlation analysis was used to analyze the relationship between miR-4429 and circ_0000069, or ZIC2 mRNA in CC tissues.

Results

Circ_0000069 was increased in CC tissues and cells

As presented in Figure 1A, circ_0000069 was upregulated in cervical cancer tissues than normal tissues with microarray analysis (GSE102686; https://www.ncbi.nlm.nih.gov/geo/query/acc.cgi?acc=GSE102686). Furthermore, the schematic model showed that circ_0000069 derived from the STIL gene exons 6 and 7 (Figure 1B). Our results also confirmed that circ_0000069 was increased in CC tissues when compared with paired normal tissues (Figure 1C). Interestingly, circ_0000069 showed higher expression in III+ IV grade than I+II grade (Figure 1D). Consistently, CC cells (HeLa and SW756) showed higher expression of circ_0000069 than HcerEpic cells. Besides, circ_0000069 was more resistant to RNase R than linear STIL mRNA (Figure 1F-1G). According to the Kaplan-Meier, CC patients with high expression of circ_0000069 had a poor overall survival when contrasted to low expression group (Figure 1H). Moreover, circ_0000069 level was associated with tumor size, the tumor, node, and metastasis (TNM) stage, and lymph node metastasis in CC patients

(Table 1). Collectively, circ_0000069 was upregulated in CC tissues and cells, and its expression was associated with poor prognosis of CC patients.

Circ_0000069 silencing inhibited proliferation, migration, and invasion while induced cell cycle arrest and apoptosis in CC cells

In subsequent experiments, HeLa and SW756 cells were transfected with si-circ_0000069 or si-NC to explore the functional role of circ_0000069 in CC. As shown in Figure 2A-2B, circ_0000069 was downregulated in HeLa and SW756 cells infected with si-circ_0000069 than si-NC group. After transfection, si-circ_0000069 obviously repressed cell proliferation in HeLa and SW756 cells with MTT assay (Figure 2C-2D). Consistently, colony formation assay results indicated that the silencing of circ_0000069 inhibited colony formation in HeLa and SW756 cells (Figure 2E). Conversely, apoptotic cells were increased in si-circ_0000069 group than that in si-NC group by performing flow cytometry assay (Figure 2F). In addition, the proportion of cells in G0/G1 phase was increased while S phase was decreased in HeLa and SW756 cells transfected with si-circ_0000069 than control group (Figure 2G-2H). To measure cell cycle and apoptosis-related proteins expression, western blot assay was conducted in transfected HeLa and SW756 cells. As displayed in Figure 2I-2J, Bax was upregulated while Bcl-2, CDK2, and CDK4 were downregulated in HeLa and SW756 cells after knockdown of circ_0000069. The results of transwell analysis indicated that treatment with si-circ_0000069 impeded migration and invasion abilities when compared to the control group (Figure 2K-2L). Therefore, knockdown of circ_0000069 could suppress CC development by mediation of proliferation, migration, invasion, cell cycle arrest and apoptosis of CC cells.

MiR-4429 was a target of circ_0000069 in CC cells

As shown in Figure 3A-3B, overexpression of circ_0000069 enhanced the pull-down efficiency of biotinylated-circ_0000069 probe. 18 potential target miRNAs were clustered in Figure 3C by starbase and circBank databases analysis. After the biotinylated-circ_0000069 probe interacting with cell lysates from HeLa and SW756 cells, we found that miR-4429 showed the highest abundance among 18 potential target miRNAs in both of HeLa and SW756 cells (Figure 3D-3E). Binding regions between circ_0000069 and miR-4429 were displayed in Figure 3F. After RNA pull-down assay, circ_0000069 was enriched in the product isolated from Biotin-miR-4429-WT group than Biotin-miR-4429-MUT group (Figure 3G-3H). The dual-luciferase assay results suggested that miR-4429 mimic repressed the luciferase activity of circ_0000069 WT than control, while luciferase activity of circ_0000069 MUT was not affected by miR-4429 mimic (Figure 3I-3J). Importantly, we also noticed that miR-4429 was decreased in CC tissues and cells than that in controls (Figure 3K-3L). MiR-4429 was negatively correlated with circ_0000069 expression in CC tissues (Figure 3M). Additionally, the silencing of circ_0000069 increased miR-4429 expression in HeLa and SW756 cells (Figure 3N). Therefore, miR-4429 was negatively regulated by circ_0000069 in HeLa and SW756 cells.

Inhibition of miR-4429 reversed the effects of circ_0000069 knockdown on proliferation, apoptosis, cell cycle, migration, and invasion in CC cells

As shown in Figure 4A-4B, the analysis results indicated that the silencing of miR-4429 attenuated si-circ_0000069-induced enhancement effects on miR-4429 expression. Importantly, MTT and colony formation assays revealed that the inhibitory effects of circ_0000069 silencing on cell proliferation were abolished in

HeLa and SW756 cells by knockdown of miR-4429 (Figure 4C-4E). In addition, miR-4429 inhibitor protected HeLa and SW756 cells from si-circ_0000069-induced apoptosis (Figure 4F). Knockdown of circ_0000069 induced cell cycle arrest in G0/G1 phase and decreased S phase, which was overturned by silencing of miR-4429 in HeLa and SW756 cells (Figure 4G-4H). The western blot results revealed that miR-4429 silencing was able to partly reverse si-circ_0000069-induced enhancement expression of Bax, along with inhibitory effects on Bcl-2, CDK2, and CDK4 expression in HeLa and SW756 cells (Figure 4I-4J). The migration and invasion abilities of HeLa and SW756 cells were wreaked by transfection with si-circ_0000069, which was dramatically abrogated by miR-4429 inhibition (Figure 4K-4L). Therefore, circ_0000069 contributed to CC progress through targeting miR-4429.

MiR-4429 regulated ZIC2 expression in CC cells

Bioinformatics database analysis predicted that miR-4429 might directly interact 3'UTR of ZIC2 mRNA (Figure 5A). After that, the results of dual-luciferase reporter assay suggested that luciferase activity of ZIC2-3'UTR-WT was declined by transfection with miR-4429 mimic in HeLa and SW756 cells, while luciferase activity of ZIC2-3'UTR-MUT was not affected by miR-4429 mimic when compared with control group (Figure 5B-5C). Additionally, we noticed that ZIC2 was increased in cervical squamous cell carcinoma and endocervical adenocarcinoma tissues than normal tissues (http://gepia.cancer-pku.cn/detail.php) (Figure 5D). Currently, we confirmed that mRNA and protein expression levels of ZIC2 were overexpressed in CC tissues and cells in comparison with controls (Figure 5E-5H). In addition, ZIC2 was negatively correlated with miR-4429 expression in CC tissues (Figure 5I). What's more, overexpression of miR-4429 suppressed ZIC2 expression in CC cells (Figure 5J-5K). All data indicated that ZIC2 was a functional target of miR-4429 in CC cells.

Upregulation of ZIC2 counteracted the effect of miR-4429 overexpression on proliferation, apoptosis, cell cycle, migration, and invasion in CC cells

The underlying regulatory mechanism between ZIC2 and miR-4429 was further investigated. As shown in Figure 6A-6D, transfection with ZIC2 into HeLa and SW756 cells abolished the inhibitory effects on ZIC2 expression induced by miR-4429 mimic. Furthermore, transfection with ZIC2 could abolish the inhibiting role of miR-4429 in CC cell proliferation by performing MTT and colony formation assays (Figure 6E-6G). In addition, overexpression of ZIC2 attenuated miR-4429 mimic-induced apoptosis in HeLa and SW756 cells (Figure 6H). For cell cycle analysis, G0/G1 phase was increased, and S phase was decreased in miR-4429-overexpressing cells, which was overturned by upregulation of ZIC2 in HeLa and SW756 cells (Figure 6I-6J). Furthermore, the expression of cell apoptosis-related proteins and cell cycle protein proteins were measured by western blot assay. Bax was increased, and Bcl-2, CDK2, and CDK4 were decreased in HeLa and SW756 cells after overexpression of miR-4429, which was overturned by overexpression of ZIC2 (Figure 6K-6L). Results of transwell assay suggested that the upregulation of ZIC2 restored the loss of migration and invasion abilities of HeLa and SW756 cells induced by overexpression of miR-4429 (Figure 6M-6N). In summary, miR-4429 regulated proliferation, apoptosis, cell cycle, migration, and invasion of CC cells by targeting ZIC2.

Circ_0000069 regulated ZIC2 expression by targeting miR-4429 in CC cells

Initially, our results confirmed that circ_0000069 was positively correlated with ZIC2 mRNA expression in CC tissues (Figure 7A). Importantly, mRNA and protein expression levels of ZIC2 were declined in HeLa and

SW756 cells after silencing of circ_0000069, which was weakened by co-transfection with si-circ_0000069 and anti-miR-4429 in HeLa and SW756 (Figure 7B-7E). We could conclude that ZIC2 was regulated by circ_0000069/miR-4429 axis in CC cells.

Knockdown of circ_0000069 inhibited CC tumor growth *in vivo*

The animal experiment was performed to explore the role of circ_0000069 in tumorigenesis *in vivo*. As presented in Figure 8A-8B, the silencing of circ_0000069 significantly suppressed the tumor growth rate and tumor weight when compared with sh-NC group. Besides, circ_0000069 and ZIC2 mRNA were decreased while miR-4429 was increased in sh-circ_0000069 group than sh-NC group (Figure 8C). Consistently, western blot assay revealed that the protein expression of ZIC2 was downregulated after silencing of circ_0000069 (Figure 8D). Therefore, the downregulation of circ_0000069 impeded CC tumor growth *in vivo* by regulating miR-4429 and ZIC2.

Discussion

Collectively, current results indicated that circ_0000069 was significantly upregulated in CC tissues and cells than the negative groups. Furthermore, the CC-associated circRNA expression profile (GSE102686) also revealed that circ_0000069 was upregulated in CC. Currently, loss-of-function assays revealed that silencing of circ_0000069 could impede proliferation, invasion, and migration, as well as induce cell apoptosis and cell cycle arrest in CC cell, at least in part, by regulating miR-4429/ZIC2 network.

Previous studies indicated that circRNAs served as biomarkers in cancer by functioning oncogenic or tumor-suppressive circRNAs [18]. However, the roles and regulatory mechanism of circ_0000069 in CC remained largely unknown. In this study, patients with high circ_0000069 expression had shorter survival time than CC patients with the low expression of circ_0000069, implying that circ_0000069 might be a promising prognostic biomarker in CC. Additionally, we found that knockdown of circ_0000069 inhibited proliferation, invasion, and migration, as well as induced cell apoptosis and cell cycle arrest at G0/G1 phase in CC. Similar effects of circ_0000069 silencing were confirmed in colorectal cancer patients [7].

Recently, numerous studies have shown that circRNAs acted biological functions by serving as sponges or competing endogenous RNAs (ceRNA) of miRNAs to regulate mRNA expression [19, 20]. In this study, we found that circ_0000069 could interact with miR-4429 in CC cells by biotinylated RNA pull-down and dual-luciferase reporter assays, which suggested that miR-4429 was a target gene of circ_0000069. Besides, the silencing of circ_0000069-induced anti-tumor effects were abolished by combination of circ_0000069 knockdown and miR-4429 inhibitor in CC cell.

MiR-4429 was demonstrated to act as an anti-tumor miRNA in many malignancies, including clear cell renal cell carcinoma [10], glioblastoma [21], and gastric cancer [22]. Therefore, we evaluated whether overexpression of miR-4429 inhibited the development of CC, and functional experiments implied that the upregulation of miR-4429 impeded CC progress by regulation of proliferation, apoptosis, cell cycle, migration, and invasion of CC cells, revealing a tumor suppressor role of miR-4429 in CC. Analogously, Wu *et al*. reported that the overexpression of miR-4429 overturned the oncogenic role of LINC00313 in papillary thyroid cancer, revealing

the anti-tumor role of miR-4429 [23]. In addition, miR-4429 could increase the radio-sensitivity of CC cell, revealing the potential therapeutic potential of miR-4429 for CC patients [11].

Moreover, overexpression of ZIC2 may be an adverse prognostic factor for oral squamous cell carcinoma patients [24]. Lu *et al*. also reported that ZIC2 expression was significantly in hepatocellular carcinoma tissues than control, which may result to poor outcomes in patients with hepatocellular carcinoma [25]. Consistently, ZIC2 was upregulated in CC tissues and cells than controls. More importantly, miRNAs were known to play a pivotal role in human diseases by targeting 3'UTR of target mRNA [9]. ZIC2 was reported as a target gene of multiple miRNA in tumor, such as miR-1271-5p [26]. Surely, a miRNA may target many genes in diseases, which may ascribe to the complexity genome and multiplex regulation network of gene expression [27, 28]. In this study, we identified ZIC2 as a putative target for miR-4429 by bioinformatics analysis. Mechanistically, ectopic expression of ZIC2 could abolish miR-4429 mimic targeting anti-oncogenes in CC, thereby promoting proliferation and inhibiting apoptosis of CC cell. Furthermore, Wang *et al*. indicated that miR-129-5p suppressed metastasis of CC cells by regulating ZIC2 [29]. In the view of ZIC2 may be contributed to CC development by regulation of the Hedgehog signaling pathway [30], thus targeted-inhibition ZIC2 may be a promising strategy for the treatment of CC.

In summary, our study demonstrated that circ_0000069 was overexpressed in CC. Functional assays suggested that circ_0000069 promotes CC progression via miR-4429 to regulate ZIC2. Therefore, circ_0000069/miR-4429/ZIC2 network may be a promising treatment approach for patients with CC.

Conclusion

In summary, our results indicated that the silencing of circ_0000069 repressed CC cells malignancy by inhibiting proliferation, migration, and invasion and including apoptosis and cell cycle arrest by regulating miR-4429/ZIC2 network. Therefore, therapy targeting circ_0000069/miR-4429/ZIC2 may be a promising treatment strategy for the treatment of human CC.

Abbreviations

CC: Cervical cancer; RT-qPCR: real-time quantitative polymerase chain reaction; circRNAs: Circular RNAs; miRNAs: MicroRNAs; ZIC2: Zinc finger protein of the cerebellum 2; siRNA: Small interfering RNA; si-NC: siRNA control; FITC: fluorescein isothiocyanate; shRNAs: short hairpin RNAs.

Declarations

Ethics approval and consent to participate

The study was approved by the Ethics Committee of The Affiliated Hospital of Qingdao University and written informed consents were collected from all patients and hospitals.

The animal experiment was permitted by the Animal Research Committee of The Affiliated Hospital of Qingdao
University and performed in accordance with the guidelines of the National Animal Care and Ethics Institution.

Consent for publication

Not applicable

Availability of data and materials

The data sets used and/or analyzed during the current study are available from the corresponding author on reasonable request.

Competing interests

The authors declare that they have no conflicts of interest.

Funding

None

Authors' contributions

Hongjuan Yang, Xiangkun Li and Xiangkun Li performed experiments, analyzed data, and wrote the manuscript. Chang Wang and Dongyan Qin designed research, performed experiments, and analyzed data. Dongmei Gao and Jinwen Jiao conceived and designed research.

Acknowledgment

Thanks for all participants involved in this study.

References

1. Bray F, Ferlay J, Soerjomataram I, Siegel RL, Torre LA, Jemal A. Global cancer statistics 2018: GLOBOCAN estimates of incidence and mortality worldwide for 36 cancers in 185 countries. CA Cancer J Clin. 2018, 68(6):394-424.
2. Goncalves A, Fabbro M, Lhomme C, Gladieff L, Extra J-M, Floquet A, Chaigneau L, Carrasco AT, Viens P. A phase II trial to evaluate gefitinib as second-or third-line treatment in patients with recurring locoregionally advanced or metastatic cervical cancer. Gynecol Oncol. 2008, 108(1):42-6.
3. Friedlander M, Grogan M. Guidelines for the treatment of recurrent and metastatic cervical cancer. Oncologist. 2002, 7(4):342-7.
4. Chen L-L. The biogenesis and emerging roles of circular RNAs. Nat Rev Mol Cell Biol. 2016, 17(4):205.
5. Chen L-L, Yang L. Regulation of circRNA biogenesis. RNA biol. 2015, 12(4):381-8.
6. Meng S, Zhou H, Feng Z, Xu Z, Tang Y, Li P, Wu M. CircRNA: functions and properties of a novel potential biomarker for cancer. Mol Cancer. 2017, 16(1):94.
7. Guo J-n, Li J, Zhu C-l, Feng W-t, Shao J-x, Wan L, Huang M-d, He J-d. Comprehensive profile of differentially expressed circular RNAs reveals that hsa_circ_0000069 is upregulated and promotes cell proliferation, migration, and invasion in colorectal cancer. Onco Targets Ther. 2016, 9:7451.

8. Sun P, Shen Y, Gong J-M, Zhou L-L, Sheng J-H, Duan F-J. A new microRNA expression signature for cervical cancer. Int J Gynecol Cancer. 2017, 27(2):339-43.
9. Bartel DP. MicroRNAs: genomics, biogenesis, mechanism, and function. cell. 2004, 116(2):281-97.
10. Pan H, Hong Y, Yu B, Li L, Zhang X. miR-4429 Inhibits Tumor Progression and Epithelial-Mesenchymal Transition Via Targeting CDK6 in Clear Cell Renal Cell Carcinoma. Cancer Biother Radiopharm. 2019, 34(5):334-41.
11. Sun H, Fan G, Deng C, Wu L. miR-4429 sensitized cervical cancer cells to irradiation by targeting RAD51. J Cell Physiol. 2020, 235(1):185-93.
12. Aruga J. The role of Zic genes in neural development. Mol Cell Neurosci. 2004, 26(2):205-21.
13. Houtmeyers R, Souopgui J, Tejpar S: Deregulation of ZIC Family Members in Oncogenesis. Adv Exp Med Biol. 2018: 329-38.
14. Hatayama M, Aruga J: Role of Zic family proteins in transcriptional regulation and chromatin remodeling. Adv Exp Med Biol. 2018: 353-80.
15. Zhang P, Yang F, Luo Q, Yan D, Sun S. miR-1284 Inhibits the Growth and Invasion of Breast Cancer Cells by Targeting ZIC2. Oncol Res. 2019, 27(2):253-60.
16. Chan DW, Liu VW, Leung LY, Yao KM, Chan KK, Cheung AN, Ngan HY. Zic2 synergistically enhances Hedgehog signalling through nuclear retention of Gli1 in cervical cancer cells. J Pathol. 2011, 225(4):525-34.
17. Shen Z, Zhao K, Du T. Du T: HOXA10 promotes nasopharyngeal carcinoma cell proliferation and invasion via inducing the expression of ZIC2. Eur Rev Med Pharmacol Sci. 2017, 21(5):945-52.
18. Chen B, Huang S. Circular RNA: An emerging non-coding RNA as a regulator and biomarker in cancer. Cancer Lett. 2018, 418:41-50.
19. Arnaiz E, Sole C, Manterola L, Iparraguirre L, Otaegui D, Lawrie CH: CircRNAs and cancer: biomarkers and master regulators. Semin Cancer Biol. 2019; 58: 90-9.
20. Mitra A, Pfeifer K, Park K-S. Circular RNAs and competing endogenous RNA (ceRNA) networks. Transl Cancer Res. 2018, 7(Suppl 5):S624-8.
21. Liu X, Chen R, Liu L. SP1–DLEU1–miR-4429 feedback loop promotes cell proliferative and anti-apoptotic abilities in human glioblastoma. Biosc Rep. 2019, 39(12).
22. He H, Wu W, Sun Z, Chai L. MiR-4429 prevented gastric cancer progression through targeting METTL3 to inhibit m6A-caused stabilization of SEC62. Biochem Biophys Res Commun. 2019, 517(4):581-7.
23. Wu W, Yin H, Hu J, Wei X. Long noncoding RNA LINC00313 modulates papillary thyroid cancer tumorigenesis via sponging miR-4429. Neoplasma. 2018, 65(6):933-42.
24. Sakuma K, Kasamatsu A, Yamatoji M, Yamano Y, Fushimi K, Iyoda M, Ogoshi K, Shinozuka K, Ogawara K, Shiiba M. Expression status of Zic family member 2 as a prognostic marker for oral squamous cell carcinoma. J Cancer Res Clin Oncol. 2010, 136(4):553-9.
25. Lu S-X, Zhang CZ, Luo R-Z, Wang C-H, Liu L-L, Fu J, Zhang L, Wang H, Xie D, Yun J-P. Zic2 promotes tumor growth and metastasis via PAK4 in hepatocellular carcinoma. Cancer Lett. 2017, 402:71-80.
26. Chen X, Yang S, Zeng J, Chen M. miR-1271-5p inhibits cell proliferation and induces apoptosis in acute myeloid leukemia by targeting ZIC2. Mol Meicine Rep. 2019, 19(1):508-14.

27. Hashimoto Y, Akiyama Y, Yuasa Y. Multiple-to-multiple relationships between microRNAs and target genes in gastric cancer. PloS one. 2013, 8(5):e62589.
28. Bonci D, Coppola V, Musumeci M, Addario A, Giuffrida R, Memeo L, D'urso L, Pagliuca A, Biffoni M, Labbaye C. The miR-15a–miR-16-1 cluster controls prostate cancer by targeting multiple oncogenic activities. Nat Med. 2008, 14(11):1271.
29. Wang Y-F, Yang H-Y, Shi X-Q, Wang Y. Upregulation of microRNA-129-5p inhibits cell invasion, migration and tumor angiogenesis by inhibiting ZIC2 via downregulation of the Hedgehog signaling pathway in cervical cancer. Cancer Biol Ther. 2018, 19(12):1162-73.
30. Yip P, Chan D, Liu V, Ngan H: Zic2 synergistically enhances Hedgehog signaling pathway in cervical cancer. AACR Annual Meeting. 2008; 12-6.

Table 1

Table 1.Correlations between hsa_circ_0000069 expression and clinical characteristics of cervical cancer patients (n = 62)

Clinicopathologic parameters	Case	hsa_circ_0000069 expression		*P* value[a]
		Low(n=31)	High(n=31)	
Age (years)				0.4151
≤40	42	19	23	
>40	20	12	8	
Tumor size				0.0096*
≤4 cm	37	24	13	
>4 cm	25	7	18	
TNM stage				0.0023*
I–II	33	23	10	
III–IV	29	8	21	
Lymph node metastasis				0.0016*
No	39	26	13	
Yes	23	5	18	

;*$P < 0.05$ [a]Chi-square test

Figures

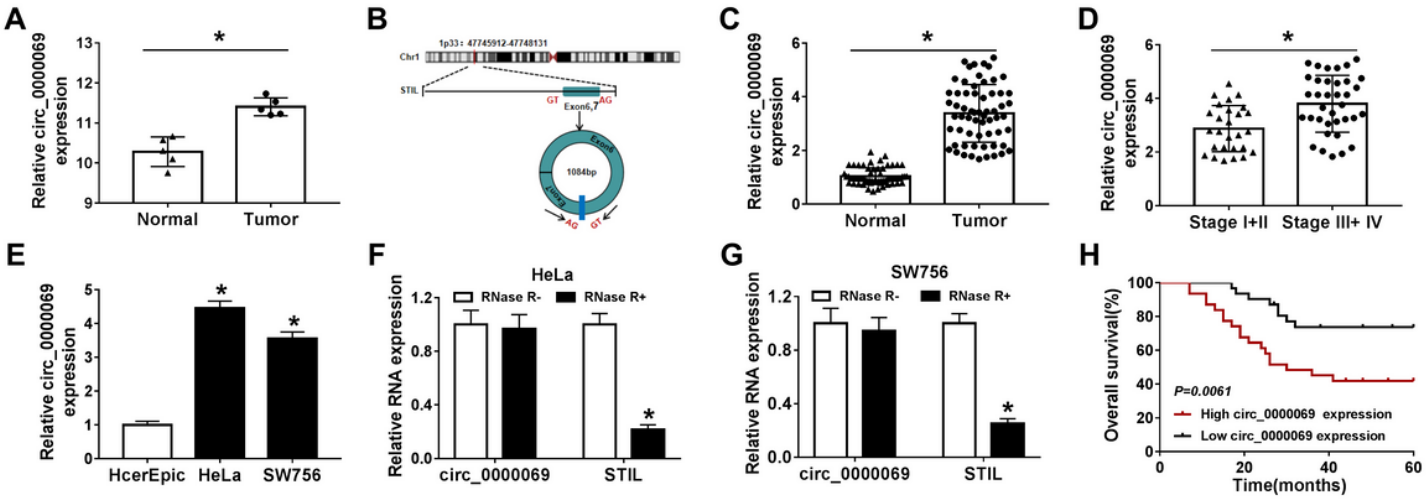

Figure 1

The expression level of circ_0000069 in cervical cancer tissues and cells. (A) The relative expression level of circ_0000069 was displayed from GEO accession: GSE102686. (B) Circ_0000069 was back-spliced by exons 6 and 7 of STIL gene. (C-D) RT-qPCR was used to measure the expression level of circ_0000069 in cervical cancer tissues (N=62) and paired normal tissues, along with I+II grade (N=26) and III+IV grade (N=36) cervical cancer tissues. (E) The relative expression level of circ_0000069 was assessed by RT-qPCR assay in HeLa, SW756, and HcerEpic cells. (F-G) The expression levels of circ_0000069 and STIL mRNA were measured by RT-qPCR assay in HeLa and SW756 cells after treatment with RNase R. (H) The survival curves of cervical cancer patients were plotted using the Kaplan-Meier analysis. *P < 0.05.

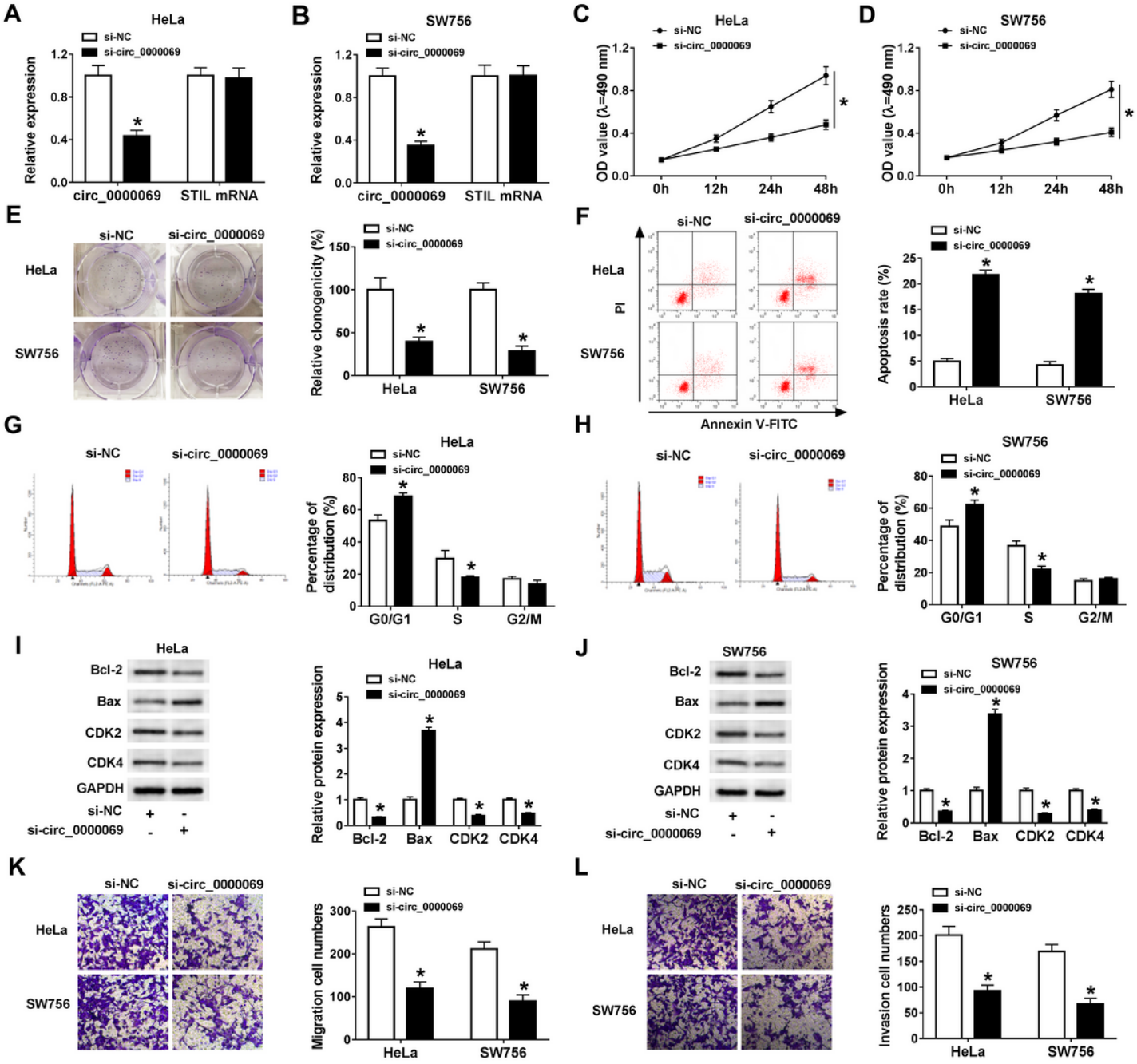

Figure 2

Effects of circ_0000069 silencing on proliferation, apoptosis, cell cycle, migration, and invasion of cervical cancer cells. (A-L) HeLa and SW756 cells were transfected with si-circ_0000069 or si-NC. (A-B) RT-qPCR assay was performed to determine the levels of circ_0000069 and STIL mRNA in HeLa and SW756 cells. (C-E) The proliferation ability of HeLa and SW756 cells was estimated by MTT and colony formation assays. (F-H) The flow cytometry assay was used to measure cell apoptosis and cell cycle distribution of HeLa and SW756 cells. (I-J) The expression levels of Bcl-2, Bax, CDK2, and CDK4 were examined by western blot assay in HeLa and SW756 cells. (K-L) Transwell migration and invasion assays were conducted in HeLa and SW756 cells. *P < 0.05.

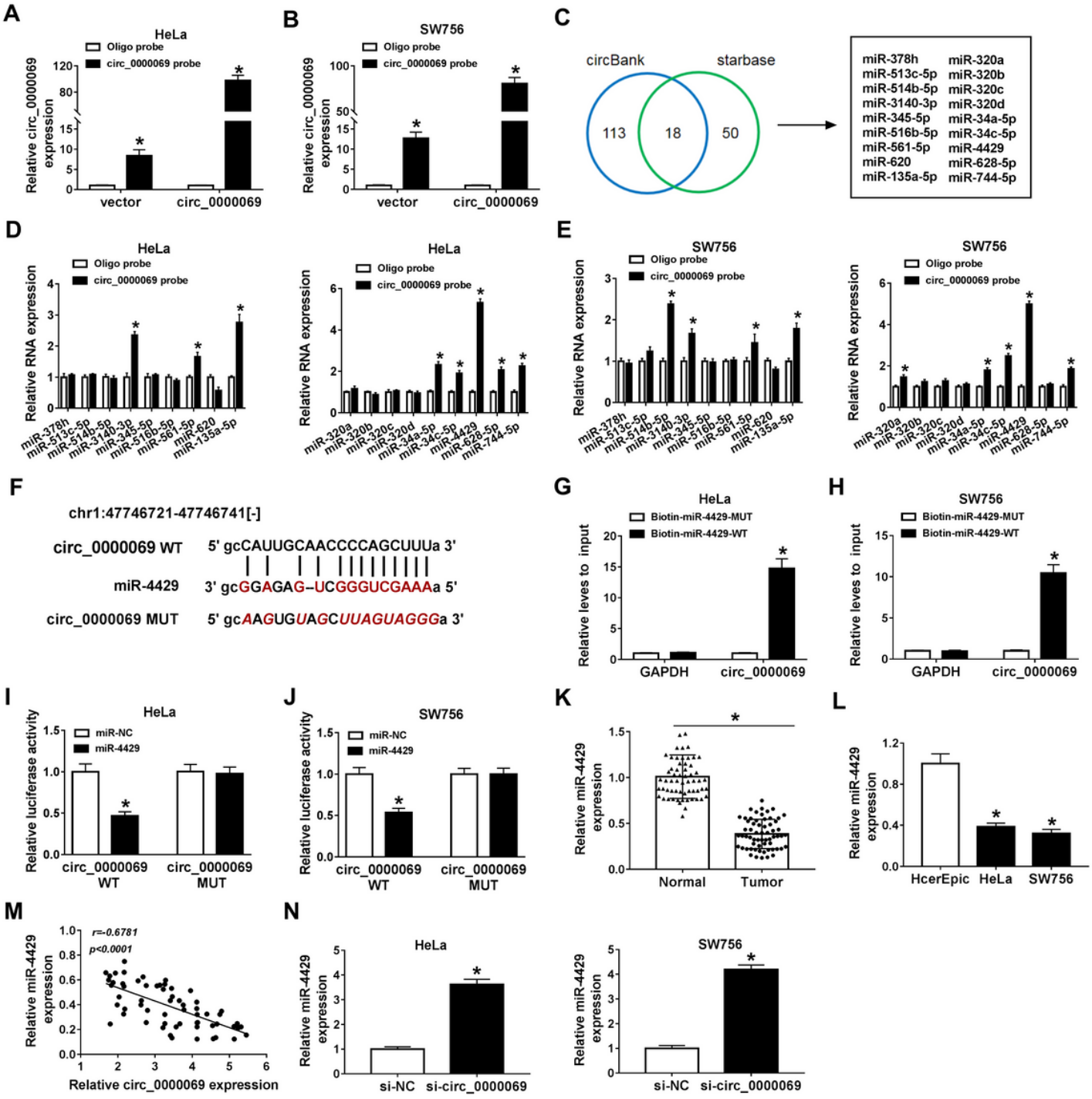

Figure 3

MiR-4429 was a direct target of circ_0000069. (A-B) The abundance of circ_0000069 was analyzed by RT-qPCR assay in lysates from HeLa and SW756 cells transfected with circ_0000069 or vector after biotinylated-circ_0000069 pull-down assay. (C) Venn diagram identified the overlap target miRNAs of circ_0000069 from starbase and circBank databases. (D-E) The expression level of target miRNAs was estimated in lysates from HeLa and SW756 cells after biotinylated-circ_0000069 pull-down assay. (F) Binding region between circ_0000069 and miR-4429, as well as matched mutant sites were shown. (G-H) The expression level of circ_0000069 was measured by RT-qPCR assay after RNA pull-down assay. (I-J) The luciferase activity was analyzed in HeLa and SW756 cells by dual-luciferase reporter assay. (K-L) The expression level of miR-4429 was measured by RT-qPCR assay in cervical cancer tissues and cells as well as matched controls. (M) The relationship between circ_0000069 and miR-4429 in cervical cancer tissues was analyzed by Pearson's correlation analysis. (N) After transfection si-circ_0000069 or si-NC into HeLa and SW756 cells, the expression of miR-4429 was measured by RT-qPCR assay. *P < 0.05.

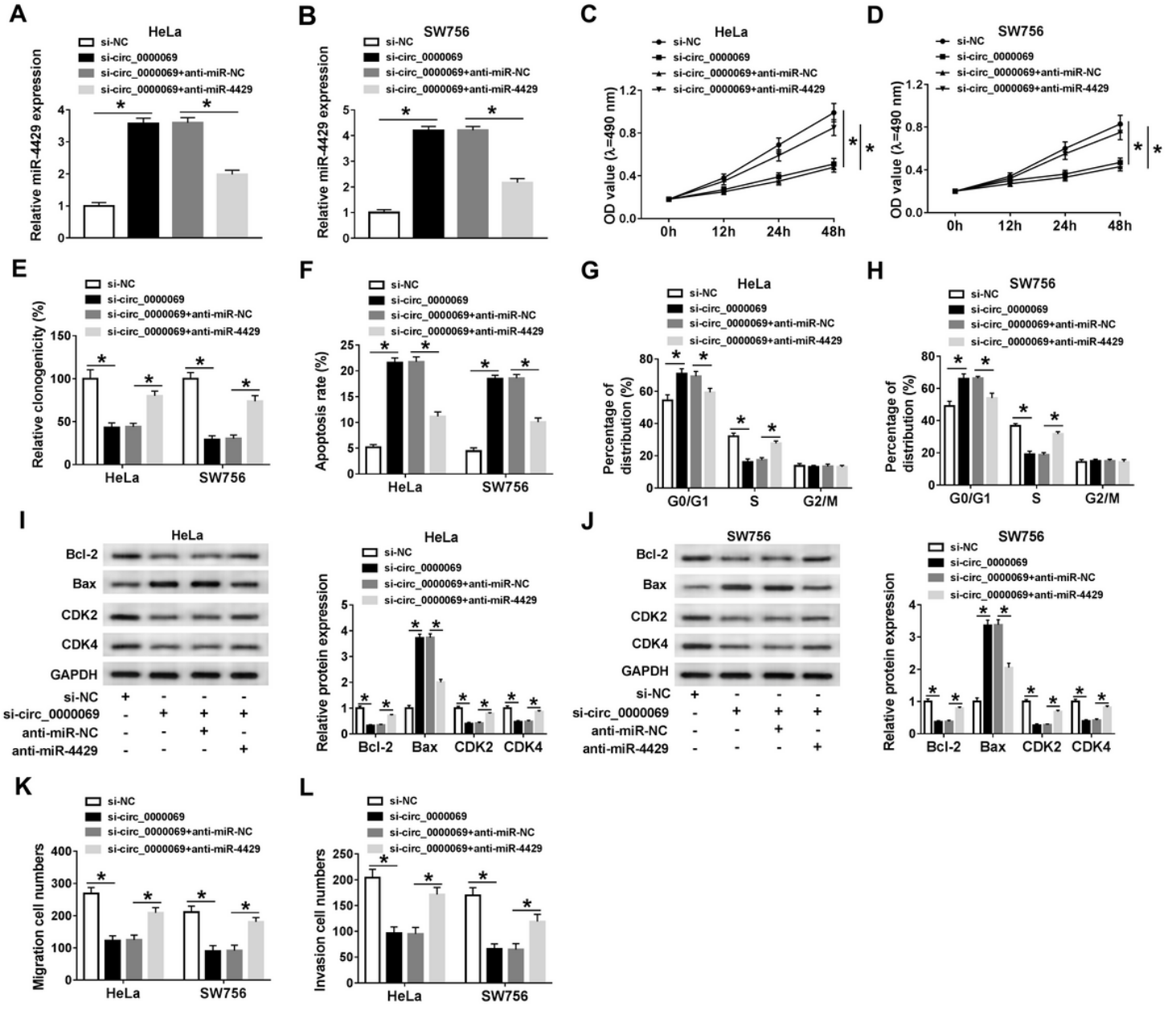

Figure 4

Knockdown of circ_0000069-induced effects on proliferation, apoptosis, cell cycle, migration, and invasion of cervical cancer cells could be abrogated by knockdown of miR-4429. (A-L) HeLa and SW756 cells were transfected with si-NC, si-circ_0000069, si-circ_0000069+anti-miR-NC, or si-circ_0000069+anti-miR-4429. (A-B) RT-qPCR was enforced to show the expression level of miR-4429 in HeLa and SW756 cells. (C-E) MTT and colony formation assays were performed for examining the proliferation capability of HeLa and SW756 cells. (F-H) The apoptosis rate and cell cycle distribution of transfected HeLa and SW756 cells were detected by flow cytometry analysis. (I-J) The protein expression levels of Bcl-2, Bax, CDK2, and CDK4 were calculated by western blot assay in HeLa and SW756 cells. (K-L) The cell numbers of migration or invasion were presented in HeLa and SW756 cells by transwell assay. *P < 0.05.

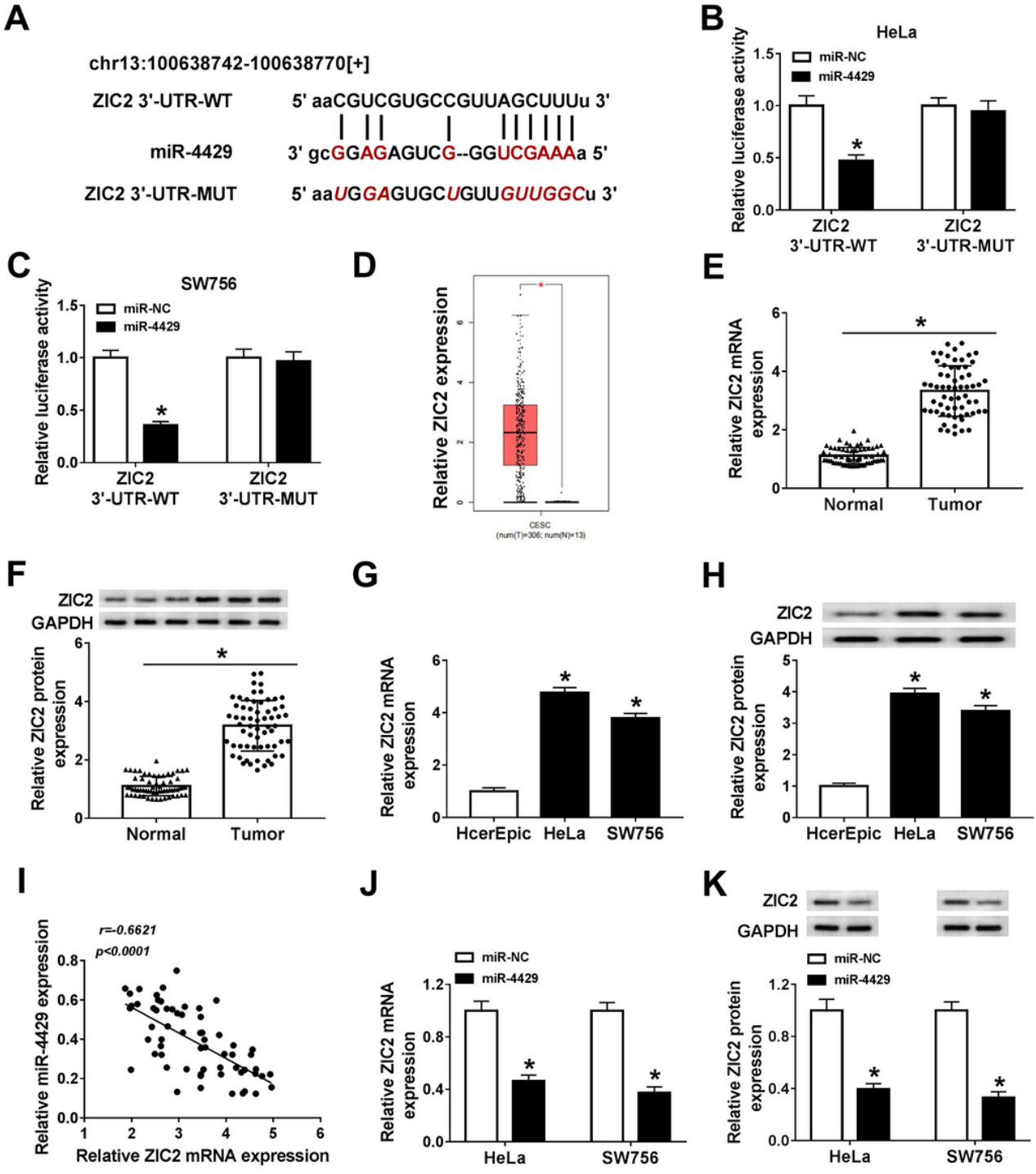

Figure 5

ZIC2 was upregulated in cervical cancer tissues and cells and it was negatively regulated by miR-4429. (A) MiR-4429 had complementary sites in 3'UTR of ZIC2 by bioinformatics analysis. (B-C) HeLa and SW756 cells were co-transfected with indicated reporter vector and miR-4429 or miR-NC for dual-luciferase reporter assay. (D) The expression levels of ZIC2 were displayed from the cancer genome atlas dataset (http://gepia.cancer-pku.cn/detail.php). (E-H) The mRNA and protein expression levels of ZIC2 in cervical cancer tissues and cells, as well as matched negative groups were measured by RT-qPCR and western blot assay, respectively. (I) Pearson's correlation analysis was introduced to show the correlation relationship between miR-4429 and ZIC2 mRNA in cervical cancer tissues. (J-K) The expression levels of ZIC2 were assessed by RT-qPCR and western blot assays in HeLa and SW756 cells transfected with miR-4429 or miR-NC. *P < 0.05.

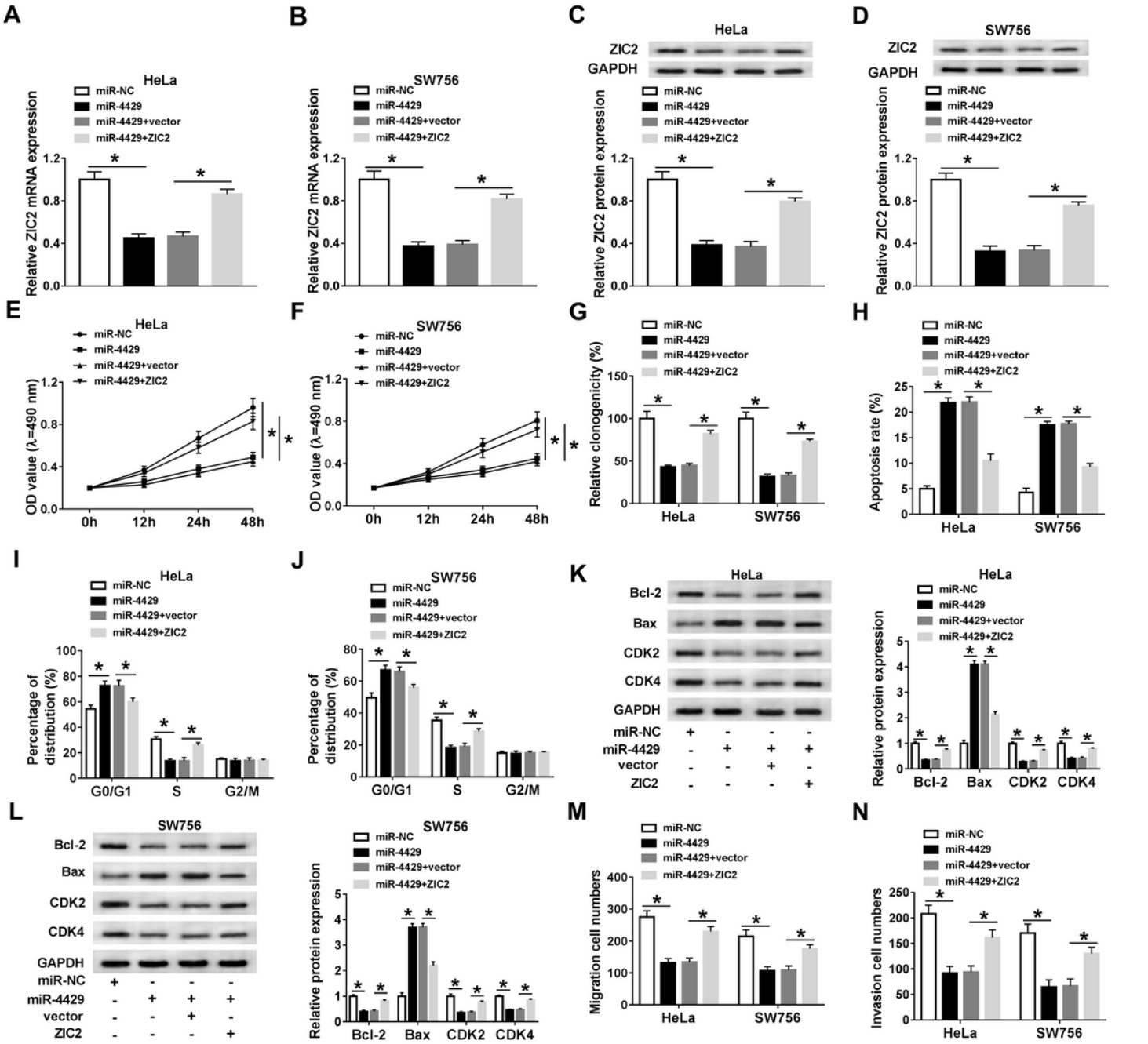

Figure 6

MiR-4429 regulated proliferation, apoptosis, cell cycle, migration, and invasion of cervical cancer cells by targeting ZIC2. (A-N) HeLa and SW756 cells were transfected with miR-NC, miR-4429, miR-4429+vector, or miR-4429+ZIC2. (A-D) The expression levels of ZIC2 in HeLa and SW756 cells were quantified by RT-qPCR and western blot assays. (E-G) The proliferation capability of transfected HeLa and SW756 cells was determined by MTT and colony formation assays. (H-J) The flow cytometry analysis was conducted to measure apoptosis rate and cell cycle distribution in HeLa and SW756 cells after transfection. (K-L) The western blot assay was performed to show Bcl-2, Bax, CDK2, and CDK4 levels in HeLa and SW756 cells post-transfection. (M-N) The transwell migration and invasion assays were used to assess the capabilities of migration and invasion of HeLa and SW756 cells. *P < 0.05.

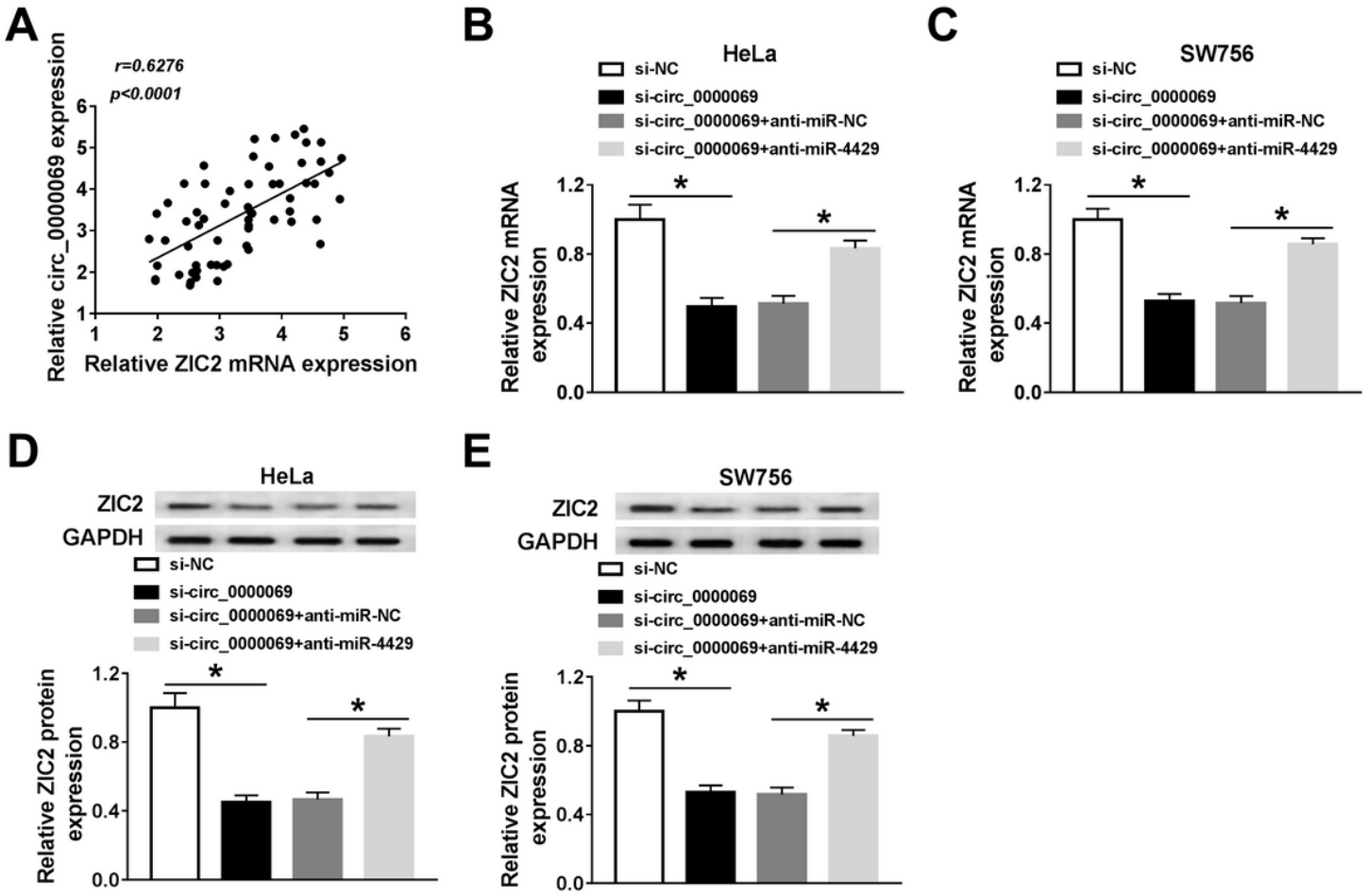

Figure 7

The expression level of ZIC2 in cervical cancer cells. (A) The correlation analysis between ZIC2 mRNA and circ_0000069 was conducted. (B-E) The mRNA and protein expression levels of ZIC2 were measured by RT-qPCR and western blot assay in HeLa and SW756 cells transfected with si-NC, si-circ_0000069, si-circ_0000069+anti-miR-NC, or si-circ_0000069+anti-miR-4429, respectively. *P < 0.05.

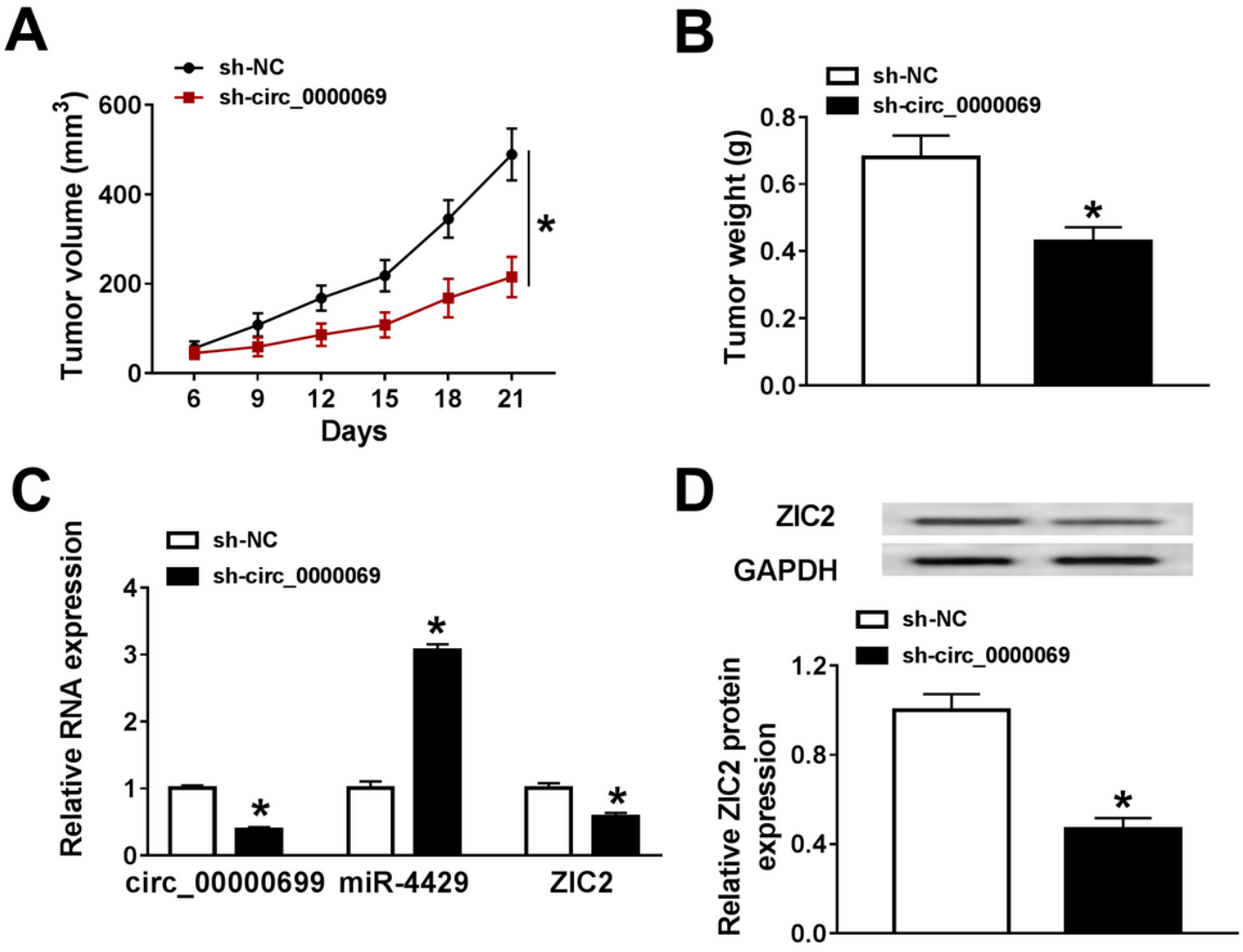

Figure 8

Silencing of circ_0000069 repressed tumor growth. (A-B) The growth curves and weight of cervical cancer tumors were shown. (C) The expression levels of circ_0000069, miR-4429 and ZIC2 mRNA in removed tumor tissues were determined by RT-qPCR assay. (D) Western blot assay was performed to show the protein level of ZIC2 in removed tumor tissues, with GAPDH as control. *P < 0.05.